

Transport Properties of a Delta-Shell Gas with Long Scattering Lengths

Sergey Postnikov* and Madappa Prakash†

Department of Physics and Astronomy,
Ohio University, Athens, Ohio 45701, USA

(Dated: May 18, 2022)

The coefficients of diffusion, thermal conductivity, and shear viscosity are calculated for a system of non-relativistic particles interacting via a delta-shell potential $V(r) = -v\delta(r-a)$ when the average distance between particles is smaller than a . The roles of resonances and long scattering lengths including the unitary limit are examined. Results for ratios of diffusion to viscosity and viscosity to entropy density are presented for varying scattering lengths.

PACS numbers: 03.75.Ss, 51.20.+d, 67.10.Jn

Gottfried's treatment [1, 2] of the quantum mechanics of two particles interacting through a delta-shell potential $V(r) = -v\delta(r-a)$, where v is the strength and a is the range, forms the basis of this work in which the transport properties of a dilute gas of non-relativistic particles are calculated for densities n for which the average inter-particle distance $d \sim n^{-1/3} \gg a$. The delta-shell potential is particularly intriguing as the scattering length a_{sl} and the effective range r_0 can be tuned at will, including the interesting case of $a_{sl} \rightarrow \infty$ that is accessible in current atomic physics experiments (see, for e.g., [3]). The delta-shell potential also allows us to understand the transport characteristics of nuclear systems in which the neutron-proton and neutron-neutron scattering lengths ($a_{sl} \simeq -23.8$ fm and -18.5 fm, respectively [4]) are much longer than the few fm ranges of strong interactions. In addition, the delta-shell potential admits resonances.

For small departures of the distribution function from its equilibrium, the net flows of mass, energy and momentum are characterized by the coefficients of diffusion, thermal conductivity and shear viscosity, respectively. Here we calculate these coefficients in first and second order of deviations using the Chapman-Enskog method [5]. In particular, we examine these transport properties for varying physical situations including the case of an infinite scattering length, i.e., the unitary limit, and when resonances are present.

We begin by collecting the two-particle quantum mechanical inputs [1, 2, 6] and cast them in forms suitable for the calculation of the transport coefficients. The Hamiltonian for two particles interacting via the delta-shell potential is $\hat{H} = -\hbar^2 \frac{\Delta}{2\mu} - v\delta(r-a)$, where μ denotes the reduced mass, $\Delta = \frac{1}{r^2} \frac{\partial}{\partial r} r^2 \frac{\partial}{\partial r} - \frac{\hat{L}^2}{r^2}$ is the Laplacian in spherical coordinates (\hat{L} is the orbital angular momentum operator), r is the separation distance, v and a are the strength and range parameters of the potential, respectively. In terms of the dimensionless variable $\rho = kr$ (k is the wave number), $E = \frac{\hbar^2 k^2}{2\mu}$, and l the orbital quan-

tum number, the general solution of Schrödinger equation is given by the spherical Bessel functions $j_l(\rho)$ and $n_l(\rho)$:

$$\psi(\rho) \equiv u(\rho)/\rho = A_l j_l(\rho) + B_l n_l(\rho). \quad (1)$$

The phase shifts δ_l are obtained through [1]

$$\tan(\delta_l) = \frac{g x j_l^2(x)}{1 + g x j_l(x) n_l(x)}, \quad (2)$$

where $x = ka$, and the single dimensionless parameter

$$g = (2\mu v/\hbar^2) a \quad (3)$$

controls *all* physical outcomes. At low energies ($l = 0$), the scattering length a_{sl} , the effective range r_0 and the shape parameter P , are defined through [7]:

$$k \cot(\delta_0) = -\frac{1}{a_{sl}} + r_0 \frac{k^2}{2} - P r_0^3 k^4 + O(k^6),$$

$$a_{sl} = \frac{ag}{g-1}, \quad r_0 = \frac{2a}{3} \left(1 + \frac{1}{g}\right) \quad \text{and} \quad P = -\frac{3}{40} \frac{g^2(3+g)}{(1+g)^3}.$$

Note that as $g \rightarrow 1$, $a_{sl} \rightarrow \infty$, but $r_0/a \rightarrow 4/3$ and $P \rightarrow 3/80$. For $l > 0$, Newton's generalization of scattering lengths and effective range parameters reads as [7]

$$k^{2l+1} \cot(\delta_l) = -\frac{1}{a_{sl}^{(l)}} + r_0^{(l)} \frac{k^2}{2} + O(k^4). \quad (4)$$

For the delta-shell potential, the $l \geq 0$ results are

$$\frac{a_{sl}^{(l)}}{a^{2l+1}} = \frac{(2l+1)}{((2l+1)!!)^2} \left(\frac{g}{g-(2l+1)} \right), \quad (5)$$

$$\frac{r_0^{(l)}}{a^{1-2l}} = \frac{2((2l+1)!!)^2}{(2l+3)(2l-1)} \left(\frac{2l-1}{g} - 1 \right). \quad (6)$$

The scattering lengths in Eq. (5) become very large for values of $g \rightarrow 2l+1$. In Fig. 1, we show a_{sl} and r_0 as functions of the strength parameter g for $l = 0$. The diverging tendencies of $|a_{sl}|$ as $g \rightarrow 1$ and $|r_0|$ as $g \rightarrow 0$

*Electronic address: sp315503@ohio.edu

†Electronic address: prakash@harsha.phy.ohiou.edu

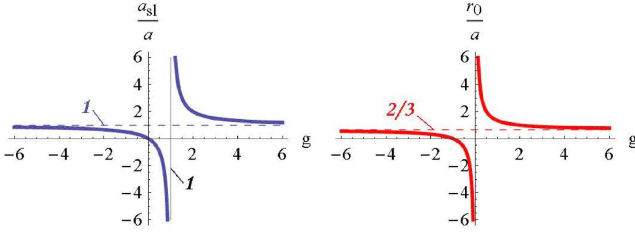


FIG. 1: (Color on-line). Scattering lengths and effective ranges as functions of the strength parameter g in Eq. (3).

are clearly evident. The case of $g \rightarrow -\infty$ corresponds to the hard-sphere case.

We turn now to calculate the coefficients of diffusion, thermal conductivity and shear viscosity, based on the Chapman-Enskog approach [5, 8]. The central ingredient is the transport cross-section of order n :

$$\phi^{(n)} = 2\pi \int_{-1}^{+1} d \cos \theta (1 - \cos^n \theta) \frac{d\sigma(k, \theta)}{d\Omega} \Big|_{c.m.}, \quad (7)$$

where the scattering angle θ and the collisional differential cross-section $\frac{d\sigma(k, \theta)}{d\Omega} \Big|_{c.m.}$ are calculated in the center of mass reference frame of the two colliding particles. For indistinguishable particles, an expansion of the cross-section in partial waves $\sum_l (2l+1)(e^{i2\delta_l} - 1)P_l(\cos \theta)$ and the orthogonality of the Legendre polynomials P_l renders the integral above to the infinite sums

$$q^{(1)} \equiv \frac{\phi^{(1)}}{4\pi a^2} = \frac{2}{x^2} \sum_l' (2l+1) \sin^2(\delta_l),$$

$$q^{(2)} \equiv \frac{\phi^{(2)}}{4\pi a^2} = \frac{2}{x^2} \sum_l' \frac{(l+1)(l+2)}{(2l+3)} \sin^2(\delta_{l+2} - \delta_l) \quad (8)$$

The prime on the summation sign indicates the use of even l for Bosons and odd l for Fermions. In Eqs. (8), the low energy hard-sphere cross section ($g \rightarrow -\infty$) $4\pi a^2$ has been used to render the transport cross sections dimensionless. If the particles possess spin s , then the properly symmetrized forms are:

$$q_{(s)}^{(n)} = \frac{s+1}{2s+1} q_{Bose}^{(n)} + \frac{s}{2s+1} q_{Fermi}^{(n)}, \quad \text{for integer } s,$$

$$q_{(s)}^{(n)} = \frac{s+1}{2s+1} q_{Fermi}^{(n)} + \frac{s}{2s+1} q_{Bose}^{(n)}, \quad \text{for half-integer } s.$$

Here, we will present results for the case of spin-1/2 particles only. The transport coefficients are given in terms of the transport integrals

$$\omega_\alpha^{(n,t)}(T) \equiv \int_0^\infty d\gamma e^{-\alpha\gamma^2} \gamma^{2t+3} q^{(n)}(x), \quad (9)$$

where $\gamma = \frac{\hbar k}{\sqrt{2\mu k_B T}} = \frac{x}{\sqrt{2\pi}} \left(\frac{\lambda(T)}{a} \right)$ with the thermal de-Broglie wavelength $\lambda = (2\pi\hbar^2/m k_B T)^{1/2}$.

In what follows, the coefficients of self diffusion \mathcal{D} , shear viscosity η , and thermal conductivity κ are normalized to the corresponding hard-sphere-like values

$$\tilde{\mathcal{D}} = \frac{3\sqrt{2}}{32} \frac{\hbar}{mna^3}, \quad \tilde{\eta} = \frac{5\sqrt{2}}{32} \frac{\hbar}{a^3}, \quad \text{and} \quad \tilde{\kappa} = \frac{75}{64\sqrt{2}} \frac{\hbar k_B}{ma^3}. \quad (10)$$

In the first order of deviations from the equilibrium distribution function, the transport coefficients are

$$\frac{[\mathcal{D}]_1}{\tilde{\mathcal{D}}} = \left(\frac{a}{\lambda(T)} \right) \frac{1}{\omega_1^{(1,1)}(T)},$$

$$\frac{[\eta]_1}{\tilde{\eta}} = \frac{[\kappa]_1}{\tilde{\kappa}} = \left(\frac{a}{\lambda(T)} \right) \frac{1}{\omega_1^{(2,2)}(T)}, \quad (11)$$

Equation (11) shows clearly that if $\omega_1^{(2,2)}$ is T -independent (as for hard-spheres with a constant cross section), the shear viscosity exhibits a $T^{1/2}$ dependence which arises solely from its inverse dependence with $\lambda(T)$. For energy-dependent cross sections, however, the temperature dependence of the viscosity is sensitive also to the temperature dependence of the omega-integral.

The second order results can be cast as

$$\frac{[\mathcal{C}]_2}{[\mathcal{C}]_1} = (1 + \delta_{\mathcal{C}}(T)) (1 \pm n\lambda^3 \epsilon_{\mathcal{C}}(T)), \quad (12)$$

where \mathcal{C} is \mathcal{D} or η or κ , and the \pm refers to Bose (+) and Fermi (-) statistics. For example,

$$\delta_\eta \equiv \frac{3(7\omega_1^{(2,2)} - 2\omega_1^{(2,3)})^2}{2 \left(\omega_1^{(2,2)} (77\omega_1^{(2,2)} + 6\omega_1^{(2,4)}) - 6(\omega_1^{(2,3)})^2 \right)},$$

$$\epsilon_\eta \equiv 2^{-7/2} \left[4 - \frac{128}{3^{3/2}} \frac{\omega_{4/3}^{(2,2)}}{\omega_1^{(2,2)}} \right]. \quad (13)$$

It is useful to define a characteristic temperature

$$\tilde{T} \equiv \frac{2\pi\hbar^2}{k_B m a^2} \quad \text{or} \quad \frac{T}{\tilde{T}} = \left(\frac{a}{\lambda} \right)^2 \quad (14)$$

in terms of which limiting forms of the transport coefficients can be studied. For spin 1/2 statistics, Fig. 2 shows $[\mathcal{D}]_1$ from Eq. (11) normalized to $\tilde{\mathcal{D}}$ from Eq. (10). As expected, the diffusion coefficient grows steadily with temperature. For $g \neq 1, 3$, and for $T \ll \tilde{T}$, we find the asymptotic behavior (the dashed lines in Fig. 2)

$$\frac{\mathcal{D}}{\tilde{\mathcal{D}}} \rightarrow 2 \left(\frac{1-g}{g} \right)^2 \sqrt{\frac{\tilde{T}}{T}}. \quad (15)$$

The cases $g \rightarrow 1, 3$ require special consideration. In these cases, the asymptotic behavior for $T \ll \tilde{T}$ is obtained from a series expansion in $x = ka$ of the transport cross sections $q^{(n)}(x)$ in Eqs. (8), and subsequent integrations of Eq. (9). We find the limiting forms:

$$\frac{\mathcal{D}}{\tilde{\mathcal{D}}} \rightarrow \begin{cases} 8\pi \left(T/\tilde{T} \right)^{3/2} & \text{for } g = 1 \\ \frac{6}{13} \left(T/\tilde{T} \right)^{1/2} & \text{for } g = 3. \end{cases} \quad (16)$$

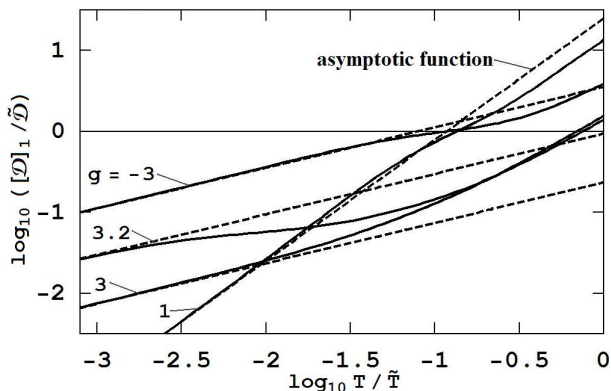


FIG. 2: Normalized (to $\tilde{\mathcal{D}}$ in Eq. (10)) diffusion coefficient as a function of normalized (to \tilde{T} in Eq. (14)) temperature for various values of the strength parameter g in Eq. (3). Solid curves show the diffusion coefficient in the first approximation, \mathcal{D}_1 in Eq. (11), and the dashed lines are its asymptotic trends for $T \ll \tilde{T}$ in Eq. (14).

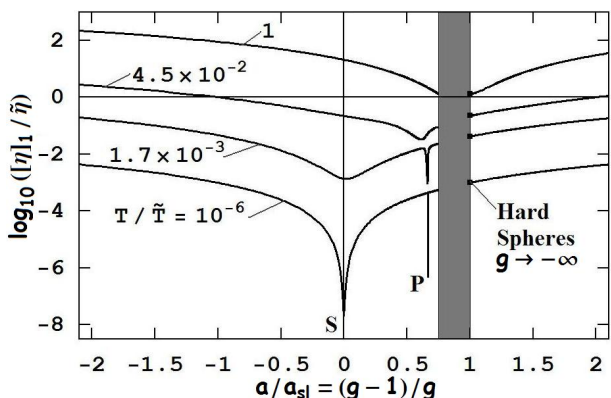


FIG. 3: (Color on-line). The normalized viscosity coefficient in Eq. (11) as a function of the inverse scattering length. Effects due to resonances associated with the partial waves $l = 0$ and 1 are indicated by the letters S and P , respectively. In the vertical shaded region, a large number of partial waves are required to obtain convergent results.

The asymptotic behavior (for $T \ll \tilde{T}$) of the shear viscosity $[\eta]_1$ is similar to that of the diffusion coefficient:

$$\frac{\eta}{\tilde{\eta}} \rightarrow \begin{cases} \left(\frac{1-g}{g}\right)^2 \left(\frac{T}{\tilde{T}}\right)^{1/2} & \text{for } g \neq 1, 3 \\ 6\pi \left(\frac{T}{\tilde{T}}\right)^{3/2} & \text{for } g = 1 \\ \frac{16}{111} \left(\frac{T}{\tilde{T}}\right)^{1/2} & \text{for } g = 3. \end{cases} \quad (17)$$

It is interesting that even at the two-body level, the coefficients of diffusion, thermal conductivity and viscosity acquire a significantly larger temperature dependence as the scattering length $a_{sl} \rightarrow \infty$ ($g \rightarrow 1$).

Figure 3 shows the normalized viscosity coefficient as a function of $\frac{a}{a_{sl}} = \frac{g-1}{g}$ for $T < \tilde{T}$. Enhanced cross sections at resonances produce significant drops in the viscosity as $g \rightarrow 2l+1$. The widths of the dips in viscosity

decrease with increasing values of l . For $T \leq \tilde{T}$, the dips become less prominent and disappear for $T \geq \tilde{T}$. For the densities and temperatures considered, the contribution from the second approximation is small as $|\delta_\eta| < 0.05$.

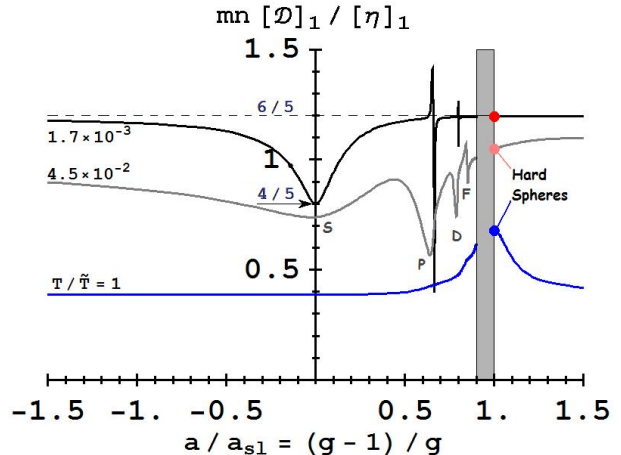


FIG. 4: (Color on-line). Ratio of diffusion (times mn) to shear viscosity versus inverse scattering length. In the vertical shaded region, a large number of partial waves are required to obtain convergent results. The hard-sphere results ($g \rightarrow -\infty$) are shown by solid circles.

g	$mn\mathcal{D}$	η	$mn\mathcal{D}/\eta$
1	$\frac{3\sqrt{2}\pi}{4} \frac{\hbar}{\lambda^3}$	$\frac{15\sqrt{2}\pi}{16} \frac{\hbar}{\lambda^3}$	$\frac{4}{5} = 0.80$
3	$\frac{9\sqrt{2}\pi}{104} \frac{\hbar}{\lambda a^2}$	$\frac{5\sqrt{2}\pi}{111} \frac{\hbar}{\lambda a^2}$	$\frac{999}{520} = 1.92$
$\neq 1, 3$	$\frac{3\sqrt{2}\pi}{8} \frac{\hbar}{\lambda a_{sl}^2}$	$\frac{5\sqrt{2}\pi}{16} \frac{\hbar}{\lambda a_{sl}^2}$	$\frac{6}{5} = 1.20$

TABLE I: First order coefficients of diffusion (times mn), shear viscosity, and their ratios for $T \ll \tilde{T}$ for select strength parameters g . The unitary limit ($g = 1$) result for η was obtained earlier in Ref. [9].

In Fig. 4, the ratio of the coefficients of diffusion (times mn) and viscosity are shown as functions of a/a_{sl} for $T \leq \tilde{T}$. As expected, the largest variations in this ratio occur as $g \rightarrow 2l+1$, that is, as resonances are approached. For $T \ll \tilde{T}$, the ratio approaches the asymptotic value $6/5$ away from resonances and $4/5$ for the S -wave resonance (a point). With increasing T , resonances become progressively broader with diminishing strengths; for $T \approx \tilde{T}$ resonances disappear. For comparison, this figure also includes results for hard spheres.

The coefficient of viscosity (as also mn times the coefficient of diffusion) has the dimension of action (\hbar) per unit volume. The manner in which the effective physical

volume \mathcal{V} changes as the strength parameter g is varied is illuminating as our results for $T \ll \tilde{T}$ in Table I shows. In the unitary limit ($g = 1$), the relevant volume is $\mathcal{V} \propto \lambda^3$. For $g = 3$, $\mathcal{V} \propto \lambda a^2$ (independent of a_{sl}), and for $g \neq 1, 3$, $\mathcal{V} \propto \lambda a_{sl}^2$ (independent of a).

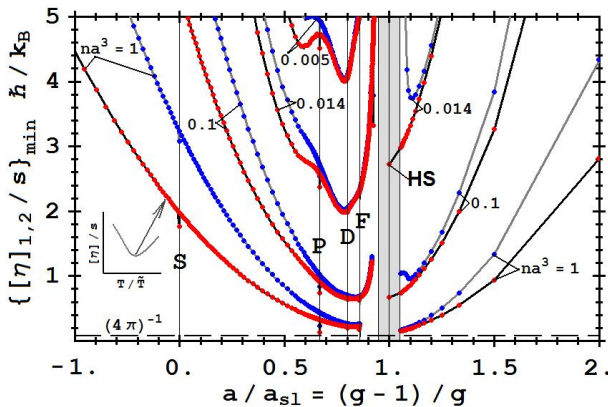


FIG. 5: (Color on-line). The insert shows the occurrence of a minimum in the ratio viscosity to entropy density versus T . For each na^3 , this minimum value in the first (lower curve) and second (upper curve) order calculations of shear viscosity is plotted versus a/a_{sl} for the indicated na^3 . In the vertical shaded region, a large number partial waves are needed. Vertical lines with letters (S, P, D , and F , respectively) indicate resonances associated with the partial waves $l = 0, 1, 2$ and 3 . The symbol HS denotes hard-spheres result for which $g \rightarrow -\infty$. The horizontal dashed line shows the conjectured lower bound $1/(4\pi)$ [10].

Recently, a lower limit to the ratio of shear viscosity to entropy density is being sought [11] with results even lower than $(4\pi)^{-1}(\hbar/k_B)$ first proposed in [10]. We therefore examine $[\eta]_{1,2}/s$ using the entropy density

$$s = (5/2 - \ln(n\lambda^3) + \delta s(T)) na^3 nk_B, \quad (18)$$

$$\delta s(T) = \left(\frac{a_2(T)}{2} - T \frac{da_2(T)}{dT} \right) \left(\frac{\lambda}{a} \right)^3,$$

which includes the second virial correction [8] to the ideal gas entropy density. The second virial coefficient [8]

$$a_2(T) = \mp 2^{-5/2} - 2^{3/2} \sum_l' (2l+1) \times \left(e^{-E_l/(k_B T)} + \frac{1}{\pi} \int_0^\infty dx \frac{\partial \delta_l}{\partial x} e^{-\xi(T)x^2} \right), \quad (19)$$

where the prime indicates summation over even l 's for Bosons ($-$) and odd l 's for Fermions ($+$), E_l is the energy of the bound state with angular momentum l and $\xi(T) = (\lambda/a)^2/(2\pi)$. The insert in Fig. 5 shows a characteristic minimum of η/s versus T for fixed dilution na^3 and strength g . Values of $[\eta]_{1,2}/s$ at the minimum are also shown functions of a/a_{sl} for several na^3 . The lower (upper) curve for each na^3 corresponds to the first (second) order calculations of η . The large role of improved estimates of η on the ratio η/s is noticeable. The case of $na^3 = 1$ possibly requires an adequate treatment of many-body effects not considered here. We can, however, conclude that in the dilute gas limit η/s for the delta-shell gas remains above $(1/4\pi)\hbar/k_B$.

Our analysis here of the transport coefficients of particles subject to a delta-shell potential has been devoted to the dilute gas (non-degenerate) limit, in which two-particle interactions dominate, but with scattering lengths that can take various values including infinity. Even at the two-body level considered, a rich structure in the temperature dependence and the effective physical volume responsible for the overall behavior of the transport coefficients are evident. The role of resonances in reducing the transport coefficients are amply delineated. Matching our results to those of intermediate and extreme degeneracies [9, 12] which highlight the additional roles of superfluidity and superconductivity reveals the extent to which many-body effects play a crucial role.

This research was supported by the Department of Energy under the grant DE-FG02-93ER40756.

-
- [1] K. Gottfried, *Quantum Mechanics, Vol. I: Fundamentals*, (W. A. Benjamin, Inc., New York, 1966), Chapter 15.
- [2] K. Gottfried, and Tung-Mow Yau *Quantum Mechanics, Vol. II*, (Springer-Verlag, New York, 2004).
- [3] J. Kinast, A. Turlapov, and J. E. Thomas, Phys. Rev. Lett. **94** 170404 (2005).
- [4] W. von Witsch et al., Phys. Lett. B **80** (1979) 187; J. Deng, A. Siepe and W. von Witsch, Phys. Rev. C **66**, 047001 (2002).
- [5] S. Chapman and T. G. Cowling, *The Mathematical Theory of Non-Uniform Gases*, (Cambridge Univ. Press, Great Britain, 1970), Chapters 9, 10 and 17.
- [6] J-P. Antoine et al, J. Phys. A: Math. Gen. **20**, 3687 (1987).
- [7] R. G. Newton, *Scattering theory of waves and particles*, (McGraw-Hill, New York, 1966), p. 311.
- [8] J. O. Hirschfelder et al, *Molecular Theory of Gases and Liquids*, (John Wiley & Sons, Inc., New York, 1967), Chapters 6 and 10.
- [9] P. Massignaan, G. M. Brun and H. Smith, Phys. Rev. A **71**, 033607 (2005); G. M. Brun and H. Smith, Phys. Rev. A **72**, 043605 (2005), Phys. Rev. A **75**, 043612 (2007).
- [10] P. Kovtun, D. T. Son and A. O. Starinets, Phys. Rev. Lett. **94**, 111601 (2005).
- [11] Y. Kats and P. Petrov, JHEP **0901**, 044 (2009); M. Brigante et al., Phys. Rev. Lett. **100**, 191601 (2008); A. Buchel et al., arXiv:0812.2521 [hep-th].
- [12] G. Rupak and T. Schäfer, Phys. Rev. A **76**, 053607 (2007).